Photochemistry and Photobiology, 2018, 94: 994–1002

Calcification Moderates the Increased Susceptibility to UV Radiation of the Coccolithophorid *Gephryocapsa oceanica* Grown under Elevated CO_2 Concentration: Evidence Based on Calcified and Non-calcified Cells

Hangbin Miao[1], John Beardall[1,2] and Kunshan Gao[1,3]*

[1]State Key Laboratory of Marine Environmental Science/College of Ocean and Earth Sciences, Xiamen University, Xiamen, China
[2]School of Biological Sciences, Monash University, Clayton, Vic, Australia
[3]Laboratory for Marine Ecology and Environmental Science, Qingdao National Laboratory for Marine Science and Technology, Qingdao, China

Received 23 July 2017, accepted 7 April 2018, DOI: 10.1111/php.12928

ABSTRACT

The physiological performance of calcified and non-calcified cells of *Gephyrocapsa oceanica* (NIES-1318) and their short-term responses to UV radiation were compared for cultures grown under present-day (LC, 400 µatm) and high pCO_2 (HC, 1000 µatm) conditions. Similar growth rates and F_v/F_m values were observed in both types of cell under LC conditions, indicating that the loss of calcification in the non-calcified cells did not lead to a competitive disadvantage under such conditions. Detrimental effects of elevated pCO_2 were observed in both cell types, with the growth rate of non-calcified cells decreasing more markedly, which might reflect a negative impact of higher cytoplasmic H^+. When exposed to short-term UV radiation, similar trends in effective quantum yield were observed in both cell types acclimated to LC conditions. Elevated pCO_2 and associated seawater chemical changes strongly reduced effective quantum yield in non-calcified cells but no significant influence was observed in calcified cells. Based on these findings and comparisons with previous studies, we suggest that the negative impact of elevated cytoplasmic H^+ would exacerbate the detrimental effects of UV radiation while the possession of calcification attenuated this influence.

INTRODUCTION

Coccolithophores belong to the phylum Haptophyta and are unicellular calcifying microalgae that not only fix carbon into biomass through photosynthesis but also assimilate carbon into calcite through calcification (1). As a result, they play a particularly important role in the global carbon cycle. The most common, cosmopolitan, coccolithophore species are *Emiliania huxleyi* and *Gephyrocapasa oceanica* which have a small cell size and are able to form extensive surface blooms, making them important players in the marine environment (2).

Calcification of coccolithophores is an energy demanding process; the coccoliths must provide some benefit to cells which outweighs the cost of production although the selective advantage that the coccoliths provide is still under debate (1,3–5). In their natural environment, coccolithophores are subjected to aspects of global change such as increasing pCO_2 levels (ocean acidification) and ultraviolet radiation (UVR; 280–400 nm). The last decade has seen intensive research on the impact of ocean acidification on calcification by coccolithophores (6), yet few studies have focused on the role of calcification in affecting the response of coccolithophores to ocean acidification, despite the ability to compare the effects between calcified and non-calcified coccolithophores from the same strain, which would be the ideal method to investigate the functions of calcification, such as their interaction with photosynthesis under ocean acidification (1).

Coccolithophore blooms mostly occur within the upper mixed layer at a depth of 10–30 m (7) and are therefore often subjected to high levels of solar radiation, including UVR. UVR can decrease phytoplankton productivity through direct damage to proteins and DNA (8) or indirectly through stimulation of oxidative stress (9). Several studies (10–13), using different degrees of calcification of coccolithophores obtained by a variety of methods, have suggested that coccoliths may play a protective role to keep cells from being damaged by high levels of UVR. Xu *et al.* obtained different levels of calcification by adjusting the Ca^{2+} concentration (14), whereas Guan *et al.* adjusted the dissolved inorganic carbon (DIC) concentration (15). However, Ca^{2+} and DIC availability are also associated with other processes, which may complicate interpretation of the effects of these treatments on calcification. Gao *et al.* obtained different calcification levels by adjusting the CO_2 concentration (16); however, the different CO_2 levels will independently influence the response of phytoplankton to UV radiation as shown in diatoms acclimated to high pCO_2, which showed greater sensitivity to UV radiation (14).

In this context, the work reported here examined the impacts of acidification and calcification on the sensitivity of a coccolithophore to UV radiation, using the response of calcified and non-calcified cells obtained from the same parent stock and then grown with different levels of pCO_2.

MATERIALS AND METHODS

Culture conditions. *Gephyrocapsa oceanica* (NIES-1318) was obtained from the National Institute for Environmental Studies (NIES, Japan), and was originally isolated from the East China Sea. One lineage, originating from a calcified parent strain, became non-calcified and was then maintained separately from the parental strain which retained the calcified

*Corresponding author's email: ksgao@xmu.edu.cn (Kunshan Gao)
© 2018 The American Society of Photobiology

phenotype. It was not determined whether these cells represented non-calcified (naked) diploid cells or scaled haploid cells. However, light microscopy observations were frequently performed from a time before the sub-strain became non-calcifying, and motility was never observed. Thus, it might be reasonable to deduce that the non-calcified cells might in fact be non-calcified diploids, as haploids would be expected to have been motile for at least for some time during these observations (15,16). Both cell types were maintained in Aquil artificial seawater medium (100 μmol N, 10 μmol P) (17) under a photon flux density of 200 μmol photons m^{-2} s^{-1} (12:12 light:dark period) in a plant growth chamber (GXZ, Ruihua, Wuhan, China) at a constant temperature of 25°C.

Experimental setup. Triplicate cultures for each cell type were grown semi-continuously in tightly closed polycarbonate bottles (500 mL, Nalgene) under present-day pCO_2 (LC, 400 μatm) for about 20 generations, then transferred to high pCO_2 (HC, 1000 μatm) for another 20 generations. During the acclimation period, the head space inside the culture bottles was minimized to avoid outgassing effects. Cell density was maintained within a range of 1.5×10^4–6.0×10^4 cells mL^{-1} by diluting the cultures with the target pCO_2 pre-equilibrated media every 24 h so that the seawater carbonate parameters were stable. The sealed cultures were shaken three times a day to ensure equal exposure to light. Growth rate, pH, cell size and maximal quantum yield were monitored for 5 days at the end of each pCO_2 acclimation.

For the investigation of short-term responses to UV radiation, triplicate samples were harvested (at the middle of the light period) and transferred to 50 mL quartz tubes to test UV effects by measuring effective quantum yield and non-photochemical quenching (NPQ) of the cells during a 48-min exposure under a solar simulator (Sol 1200W, Dr. Hönle, Martinsried, Germany). The quartz tubes were covered with three different types of cut-off foil (395 nm cut-off foil, transmitting irradiances above 395 nm; 320 nm cut-off foil, transmitting irradiances above 320 nm; 295 nm cut-off foil, transmitting irradiances above 295 nm) ensuring the cells were exposed to PAR (P), PAR + UVA (PA) and PAR + UVA + UVB (PAB), respectively. The average irradiances of PAR, UVA and UVB in the solar simulator were 167.7 (800 μmol photons m^{-2} s^{-1}), 67.8 and 3.2 W m^{-2}, respectively, and the temperature (25 °C) was controlled by a cooling circulator (CAP-3000, Rikakikai, Japan). Pigment contents, particulate organic carbon (POC), particulate inorganic carbon (PIC) contents and relative electron transport rate (rETR) were also measured at the end of each pCO_2 treatment.

Measurement of radiation. The light intensity was measured with a radiometer (PAM 2100, solar light) that has channels for UVB, UVA and PAR.

Measurement of carbonate chemistry. The pH in the cultures was measured with a pH meter (Benchtop pH510, OAKTON) that was calibrated with National Bureau of Standards (NBS) buffer solution (Hanna). Other related parameters of the carbonate chemistry were calculated using the software CO2SYS (18), according to known values of pH, salinity, nutrients and pCO_2. The equilibrium constants K_1 and K_2 for the carbonic acid dissociation, used for all calculations, were according to Roy *et al.* (19).

Measurement of growth rate and cell size. The concentrations and diameters of cells were measured with a Coulter particle counter and size analyzer (Z-2, Beckman) before and after dilution (at the end of the light period). The specific growth rate (μ) was calculated as $\mu = (\ln N_2 - \ln N_1)/(T_2 - T_1)$, where N_2 and N_1 represent the cell concentrations at T_2 (before dilution) and T_1 (after the previous dilution) times, respectively.

Measurement of fluorescence parameters. Photochemical performance was investigated using a pulse-amplitude-modulated fluorometer (Multicolor PAM, Walz). The maximum quantum yield of PSII was calculated as $F_v/F_m = (F_m - F_o)/F_m$, Where F_o is the basal fluorescence under a measuring light (0.3 μmol photons m^{-2} s^{-1}) and F_m is the maximal fluorescence determined with a saturating pulse (3300 μmol photons m^{-2} s^{-1} for 0.8 s) in dark-adapted cells (15 min). The effective quantum yield (Y_{PSII}) was measured as $F_v'/F_m' = (F_m' - F_t)/F_m'$, where F_t is the steady-state fluorescence and F_m' is the maximal fluorescence of light-adapted cells (800 μmol photons m^{-2} s^{-1}). The rETR was calculated as $rETR = Y_{PSII} \times PAR \times 0.5$. Non-photochemical quenching (NPQ) was calculated as $NPQ = (F_m - F_m')/F_m'$. The inhibition of PSII due to UVA or UVR was calculated as $InhUVA\ (\%) = (Y_{PSII}P - Y_{PSII}PA)/(Y_{PSII}P) \times 100$ and $InhUVR\ (\%) = (Y_{PSII}P - Y_{PSII}PAB)/(Y_{PSII}P) \times 100$, respectively. The rates of UV-induced damage to the photosynthetic apparatus (k, in min^{-1}) and repair (r, in min^{-1}) were calculated according to Heraud & Beardall (20), using the Kok model that assumes simultaneous operation of the damage and recovery processes during the photoinhibitory exposures, and is calculated as follows: $Y_n/Y_0 = r/(r + k) + k/(r + k) \times e^{-(r + k) \times t}$, where Y_n and Y_0 represent Y_{PSII} at time T_n and T_0, respectively.

Measurement of pigment contents. Samples were harvested by filtering 80–100 mL of culture onto a Whatman GF/F filter (diameter: 25 mm) and extracted in 5 mL absolute methanol for 24 h at 4 °C, followed by centrifugation for 10 min (6000 g). The absorption spectrum of the supernatant was obtained by scanning the samples from 250 to 800 nm with a scanning spectrophotometer (DU 800, Beckman Coulter Inc). Chl *a*, Chl *c* and carotenoid contents were calculated using the equations of Porra (21), Ritchie (22) and Strickland & Parsons (23), respectively.

Measurement of PIC and POC. Samples for cellular POC and PIC contents were harvested by filtering 80 mL of culture onto pre-combusted (450 °C for 5 h) Whatman GF/F filters (25 mm), and then frozen at −20 °C. For particulate organic carbon (POC) analysis, inorganic carbon was removed by fuming the filters over HCl for 24 h, whereas samples for total particulate carbon (TPC) analysis were not treated with HCl. All samples were dried for 24 h and analyzed using a Perkin Elmer Series II CHNS/O Analyzer 2400 instrument (Perkin Elmer Waltham, MA). PIC was determined as the difference between POC and TPC.

Data analysis. Data were analyzed using SPSS v18.0 software. Prior to the statistical analyses, data were tested for normality and homoscedasticity. The student's *t*-test was used to analyze significant differences between cell types or CO_2 concentrations. One-way ANOVA and LSD tests were used to determine the significance of differences between light treatments. A Three-way ANOVA was also performed to examine the significant difference of the interaction effects among light treatments, CO_2 levels and cell types on damage and repair rate. The significance level was set at 0.05.

RESULTS

Carbonate system

The pH in the LC or HC cultures was significantly different as shown in Table 1. In the HC cultures, DIC, HCO_3^- and CO_2 levels were significantly higher, by 8.7%, 14.7% and 150.0%, respectively, and that of CO_3^{2-} was lower by 47.3% compared to LC cultures. No significant difference in the total alkalinity was observed between LC and HC conditions.

Growth rate and fluorescence parameters

The specific growth rates of calcified cells were similar to those of non-calcified cells under LC conditions (Fig. 1a). The growth rates of both cell types were lower when transferred to HC conditions, with the growth of non-calcified cells decreasing more than that of calcified cells ($P < 0.05$) (Fig. 1b). The maximal quantum yield (F_v/F_m) of both cell types stabilized at a value of around 0.625 under both CO_2 conditions (Fig. 1c,d). Calcified cells had a significantly higher maximal electron transport rate ($rETR_{max}$) and light saturation parameters (I_k) compared to non-calcified cells under both CO_2 conditions. When transferred from LC to HC conditions, both cell types showed a marked decrease in $rETR_{max}$ (Fig. 2).

POC and PIC contents

For non-calcified cells, no significant cellular PIC content was detected under the two CO_2 conditions. However, for calcified cells, the cellular PIC was about 60% higher ($P < 0.05$) in LC-

grown than in HC-grown cultures (Fig. 3). Elevated pCO_2 significantly (by 15%) reduced POC content in calcified cells ($P < 0.05$) while no significant difference was observed in non-calcified cells.

Diameter and pigment contents

The diameters of both cell types showed no significant differences between LC and HC conditions (Fig. 4a). Non-calcified cells had significant increases in Chl *a*, Chl *c* and carotenoid contents ($P < 0.05$), whereas calcified cells showed no significant differences in these parameters, when transferred from LC to HC conditions (Fig. 4b–d). The pigment contents did not show a significant difference between the two types under either CO_2 condition.

Effects of acute UVR exposure

The effective quantum yield, for both cell types under each CO_2 condition, decreased significantly within the first 15 min in the solar simulator, then leveled off during the rest of the 48 min exposure (Fig. 5). Regardless of the cell type and pCO_2 level, the asymptotes of the effective quantum yield were always lowest under the PAB treatment and highest under the P treatment, indicating a major influence of UVR on the photochemical performance of the cells. Although similar asymptotes in yield were observed in non-calcified and calcified cells under LC conditions, significant differences were observed in cells transferred to HC conditions (Fig. 5c,d). For non-calcified cells, the final yield asymptotes decreased considerably under UVR treatments (the final yield ratio (HC/LC) was 0.73, 0.20 and 0 for P, PA and PAB treatment, respectively (Fig. 5e)), leading to a higher UVR inhibition (the final inhibition ratio (HC/LC) was 1.58 and 1.43 for UVA and UVR (Fig. 6c)) when cells were transferred from LC to HC conditions. In contrast, for calcified cells, increased pCO_2 did not significantly affect the final yield asymptotes (Fig. 5f). The NPQ values of non-calcified cells were higher than those of calcified cells under both CO_2 levels, and no significant change was observed between HC- and LC-grown cells (Fig. 7).

The rates of damage and repair during the exposures, estimated from the changes of effective quantum yield over time under different radiation treatments, are presented in Fig. 8 and

Table 1. Values for the carbonate system for calcified and naked cells grown under LC (400 μatm CO_2) and HC (1000 μatm CO_2) conditions. Data are means ± standard deviation, $n = 3$.

pCO_2	pH_{NBS}	CO_2 (μmol kg^{-1})	HCO_3^- (μmol kg^{-1})	CO_3^{2-} (μmol kg^{-1})	DIC (μmol kg^{-1})	TA (μmol kg^{-1})
LC-naked	8.15 ± 0.01	11.32	1636.64 ± 21.84	202.06 ± 5.41	1850.03 ± 27.25	2144.78 ± 33.68
LC-calcified	8.16 ± 0.01	11.32	1649.25 ± 21.84	205.19 ± 5.41	1865.76 ± 27.25	2164.22 ± 33.68
HC-naked	7.82 ± 0.01	28.30	1899.37 ± 43.73	108.88 ± 5.01	2036.56 ± 48.74	2175.70 ± 55.77
HC-calcified	7.81 ± 0.01	28.30	1870.22 ± 24.96	105.54 ± 2.83	2004.07 ± 27.78	2139.20 ± 31.19

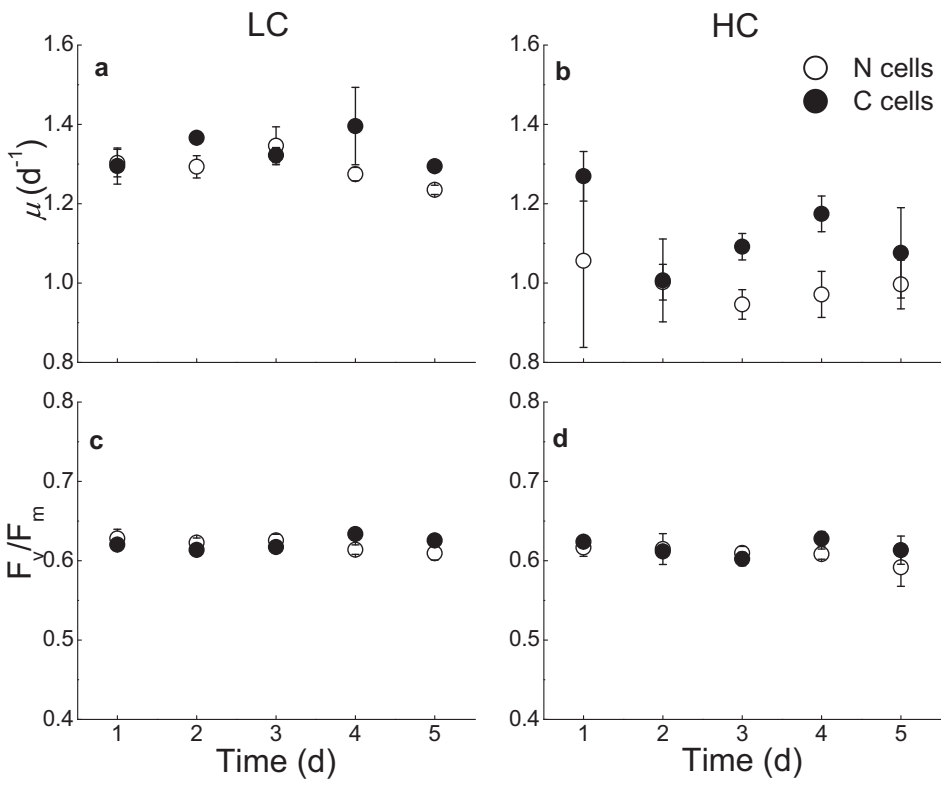

Figure 1. Specific growth rate (a, b) and F_v/F_m (c, d) of naked and calcified cells grown under LC (400 μatm CO_2) and HC (1000 μatm CO_2) conditions. The vertical lines indicate SD ($n = 3$).

Table S1. Generally, the repair rate and damage rate for calcified cells increased simultaneously when they were transferred from LC to HC conditions, leading to a similar *r*: *k* ratio at each radiation treatment. For non-calcified cells, HC-grown cultures had a lower repair rate (especially under PAB, $P < 0.05$) and a higher damage rate compared to LC-grown cultures (especially under PAB, $P < 0.05$), resulting in a decrement of the *r*: *k* ratio.

DISCUSSION

Recent work has shown that both ocean acidification and calcification would influence the physiological responses of coccolithophores to UV radiation (11,12). However, ocean acidification also affects the calcification process, which might complicate interpretation of studies to estimate the impact of calcification and ocean acidification on the response to UV radiation. Therefore, in the present work, differences in physiological performance between calcified and non-calcified cells of *Gephyrocapsa oceanica* (NIES-1318) and their short-term responses to UV radiation were measured under two levels of pCO_2, making it possible to dissect the impact of acidification and calcification on the sensitivity of coccolithophores to UV radiation. It should be recognized in this context though that although we believe, for reasons stated in the Methods, that both sets of cells were diploid, we did not test ploidy directly, so cannot state definitively that these cells represented non-calcified (naked) diploid cells or scaled haploid cells. While calcifying diploid cells would be expected to be physiologically more similar to calcifying diploid cells in traits unrelated to calcification, and thus the best control, haploid and diploid cells of Emiliania huxleyi display many different physiological traits which may suit them to different ecological niches (24–27), complicating interpretations. Keeping in mind the

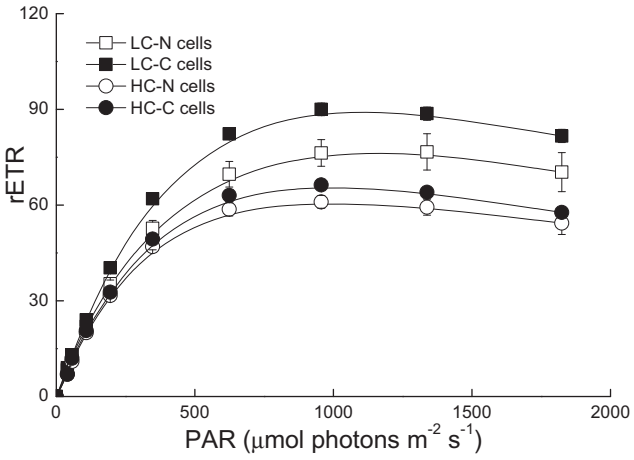

Figure 2. Rapid light curves for calcified and naked cells grown under LC (400 μatm CO_2) and HC (1000 μatm CO_2) conditions. The vertical lines indicate the SD ($n = 3$).

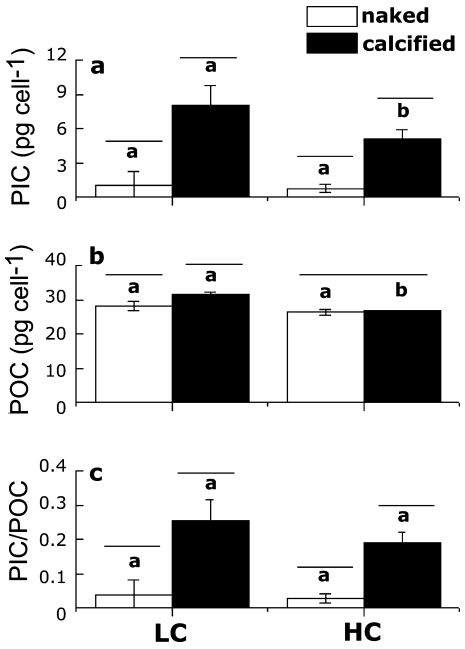

Figure 3. PIC content (a) POC content (b) and PIC/POC ratio (c) of calcified and naked cells grown under LC (400 μatm CO_2) and HC (1000 μatm CO_2) conditions. Continuous lines above histogram bars indicate a lack of significant differences between naked and calcified cells, and different letters indicate significant differences between LC and HC conditions. The vertical lines indicate SD ($n = 3$).

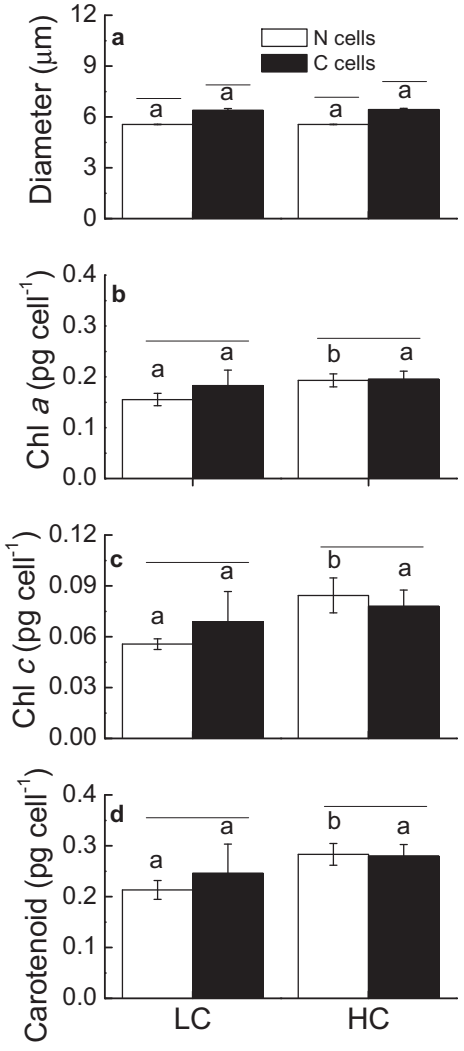

Figure 4. Diameter (a) and contents of Chl a (b), Chl c (c) and carotenoids (d) of naked and calcified cells grown under LC (400 μatm CO_2) and HC (1000 μatm CO_2) conditions. Continuous lines above histogram bars indicate a lack of significant differences between naked and calcified cells, and different letters indicate significant differences between LC and HC conditions. The vertical lines indicate SD ($n = 3$).

caveat, our data nevertheless show important differences in UVB sensitivity between calcified and non-calcified cells.

Cell division rate is a key factor in determining ecological fitness (5). In our experiments, growth rate ($P > 0.05$) and F_v/F_m ($P > 0.05$) appear to be similar between calcified and non-calcified cells under LC conditions, indicating that the loss of calcification in the non-calcified cells did not lead to a competitive disadvantage under such conditions. However, under LC conditions, a higher rETR was observed in calcified cells than in non--calcified cells, demonstrating a more efficient utilization of incident light energy than in non-calcified cells, which seems contrary to the growth rate results discussed above. This decoupling was possibly due to the higher energy demand of calcified cells to operate the calcification process.

The effects of OA can be separated into effects on carbonation (increased [CO_2] and [HCO_3^-]) as well as acidification (decreased pH) (28), with the former leading to a positive effect on phytoplankton and the latter a negative effect (29). In our study, detrimental effects of OA on both cell types were observed, as both cell types showed decreased growth rate, rETR and POC quotas when transferred to elevated pCO_2. Therefore, the negative effect of acidification must outweigh any positive effect of carbonation in our case. These findings are in line with those of Langer *et al.* (30), who found comparable responses in *E. huxleyi* strains RCC 1212 and RCC 1216. However, an increment of growth rate was previously shown in the same strain when transferred from LC to HC conditions (31); the discrepancy might originate from the different light intensity (200 vs. 100 μmol photons m^{-2} s^{-1}) used for cell growth, since several studies have reported that the balance between the effects of carbonation and acidification was strongly modulated by light (24,28,32). For example, Zhang *et al.* showed a decreased growth rate of *G. oceanica* (RCC 1303) with elevated pCO_2 at 200 μmol photons m^{-2} s^{-1} (the same light intensity used in our study) (32), which is in agreement with our findings, whereas POC quotas showed a contrary trend. Since growth rate and POC quotas at 400 μmol photons m^{-2} s^{-1} in the study of Zhang *et al.* showed a similar trend to our findings, the discrepancy could be attributed to the strain-specific light-modulated effects of ocean acidification on the coccolithophore.

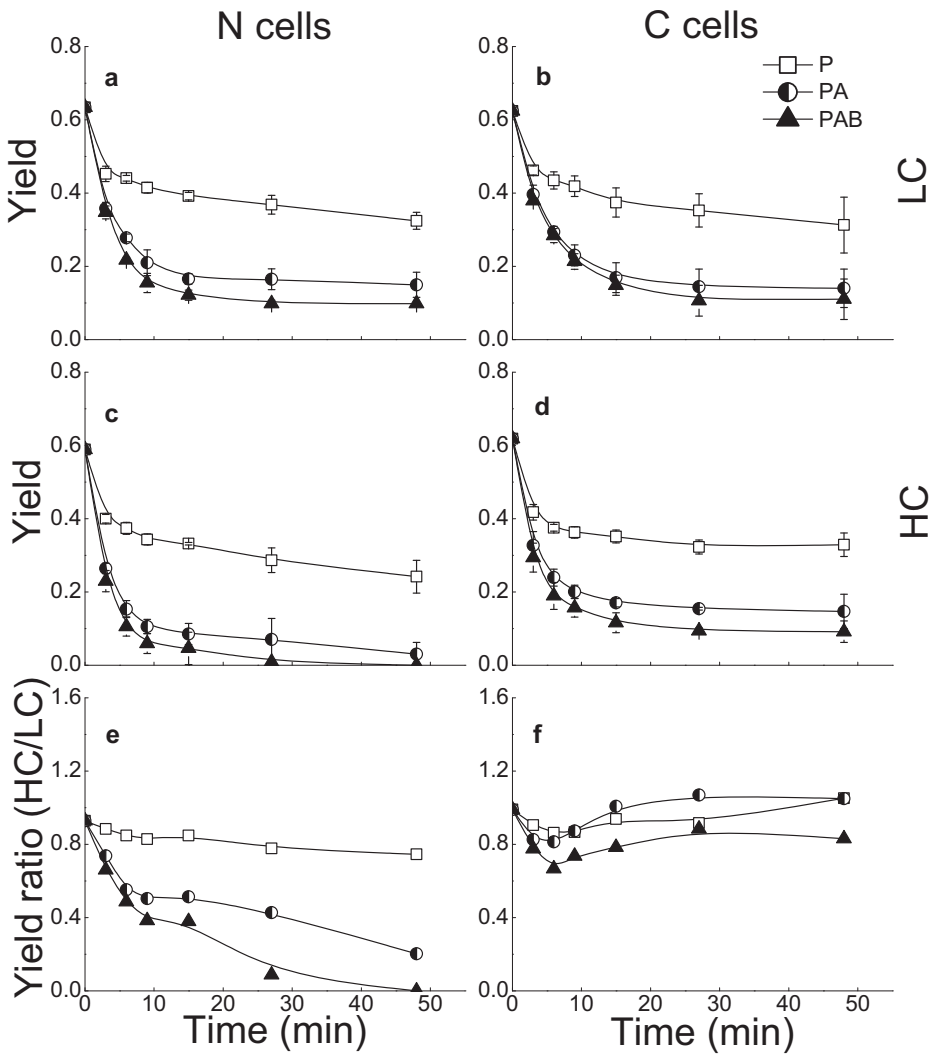

Figure 5. Time course of changes in effective quantum yield (a–d) and the yield ratio (HC/LC) (e, f) of naked and calcified cells grown under LC (400 μatm CO_2) or HC (1000 μatm CO_2) conditions while exposed to a solar radiation simulator under P, PA and PAB treatments. The vertical lines indicate SD ($n = 3$).

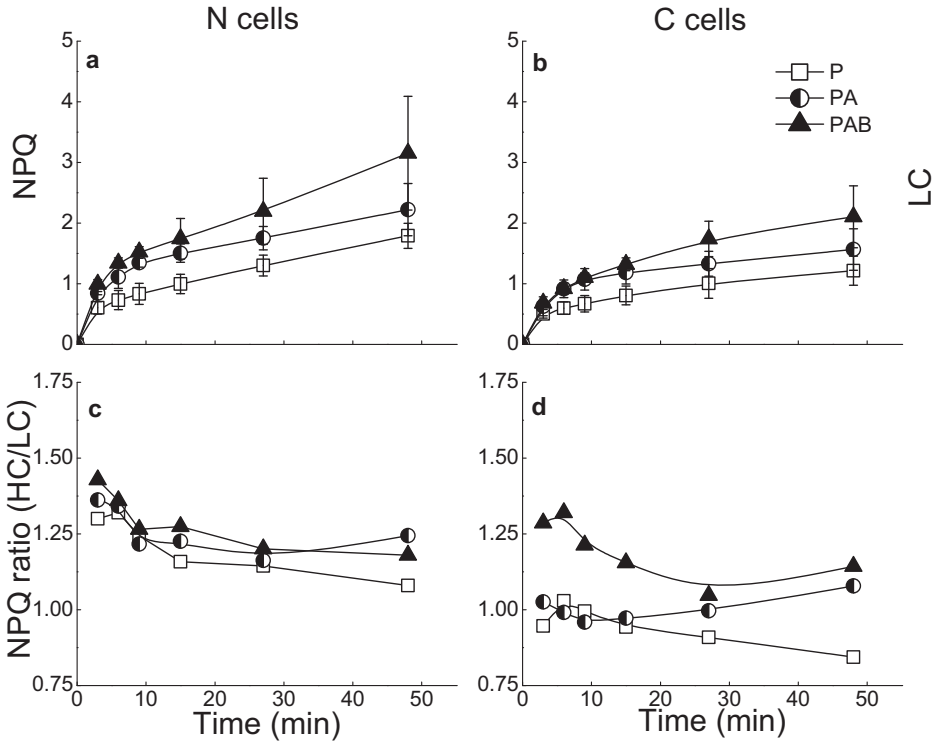

Figure 6. Time course of the decrease, relative to cells exposed to PAR only, in effective quantum yield caused by UVA and UVR for naked and calcified cells (a, b) grown at LC (400 µatm CO_2) and the changes of inhibition ratio (HC/LC) (c, d) for these cell types while exposed to a solar radiation simulator under PA and PAB treatments. The vertical lines indicate SD (n = 3).

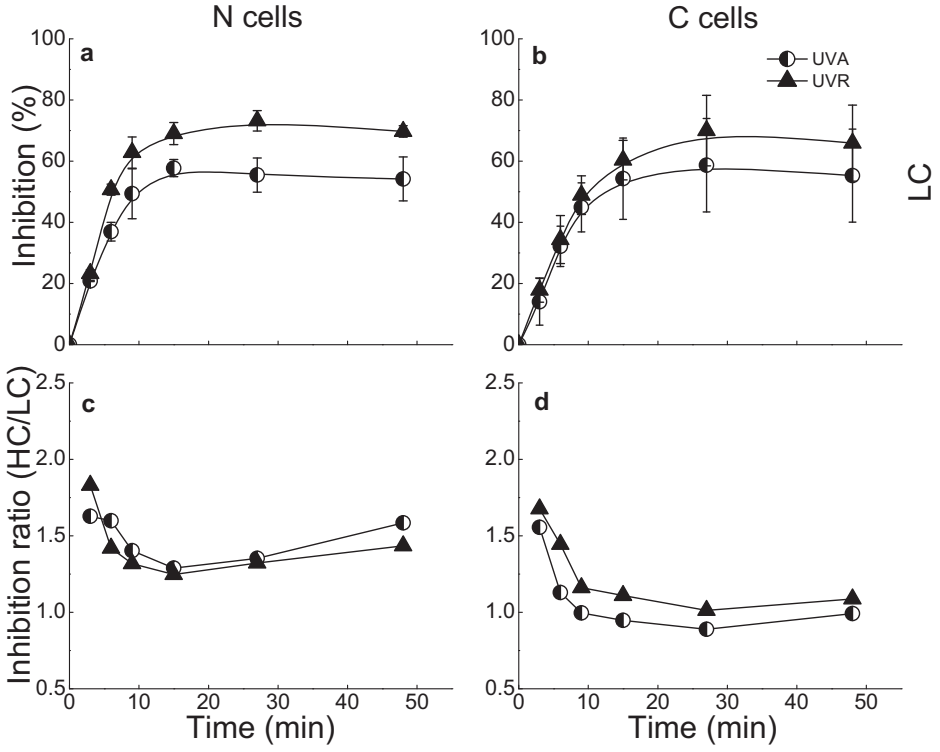

Figure 7. Time course of changes in NPQ (a, b) of naked and calcified cells grown at LC (400 µatm CO_2) and changes in the NPQ ratio (HC/LC) (c, d) of naked and calcified cells while exposed to a solar radiation simulator under P, PA and PAB treatments. The vertical lines indicate SD (n = 3).

Nevertheless, production of excreted organic carbon, such as extracellular polysaccharides, could be responsible for the observed discrepancy in POC quota (33).

It is worth noting that the OA effects were typically more pronounced in the non-calcified cells, as a 22.9% decrement of growth rate was observed in non-calcified cells while only a

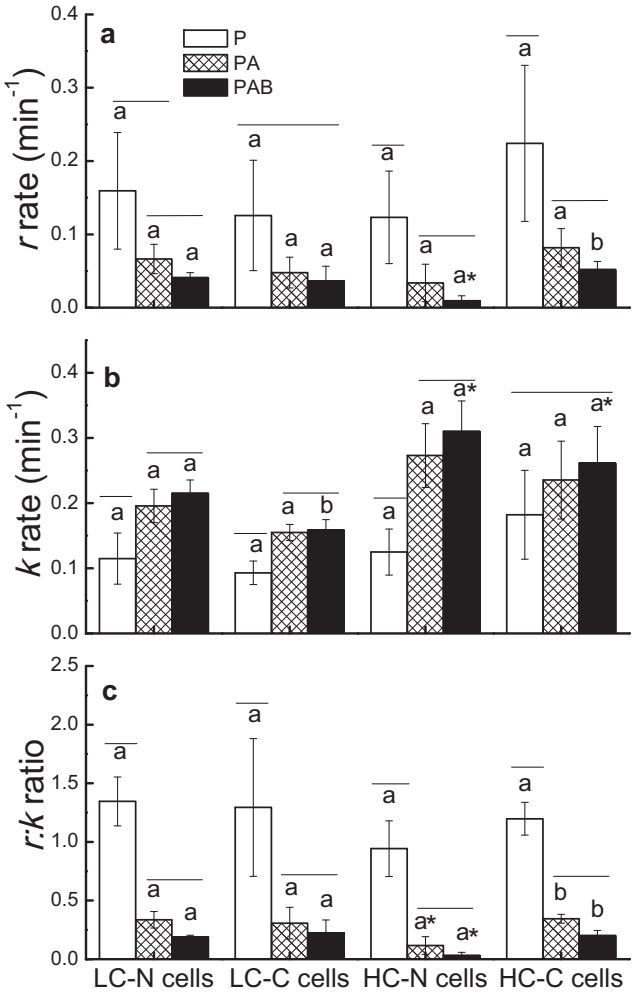

Figure 8. Rates of repair *r* (a) and damage *k* (b) and the ratio of *r: k* (c) of naked and calcified cells grown at LC (400 μatm CO_2) and HC (1000 μatm CO_2) conditions while exposed to a solar radiation simulator under P, PA and PAB treatments. Continuous lines above histogram bars indicate a lack of significant differences among P, PA and PAB treatments, different letters indicate significant differences between naked and calcified cells, asterisks indicate significant differences between LC and HC conditions. The vertical lines indicate the SD (n = 3).

15.7% reduction in calcified cells was recorded when cultures were transferred to elevated pCO_2. This suggests that calcification might play some protective role against the impacts of acidification. Suffrian *et al.* observed that cytoplasmic pH changed linearly with bulk seawater pH perturbations in decalcified *E. huxleyi* (34); however, what ultimately affects organisms is the environment at their proximate surface (35). The variation between proximate seawater pH and bulk seawater pH would be greater either because of an the increase in the thickness of the diffusive boundary layer (a positive correlate with the size of the organism (36)), or directly because of the properties of the cell wall (37). In our study, calcified cells possessed a cell wall bearing coccoliths so that the diameter (with coccoliths) was 15.3% larger than that of non-calcified cells, which might therefore ameliorate the negative effect of bulk seawater pH and prevent disruption of cellular pH homeostasis compared to the situation in the smaller diameter non-calcified cells. When transferred to elevated pCO_2, the cellular pigment content increased significantly in non-calcified cells, while no noticeable increment was observed in calcified cells. Since cytoplasmic pH affects the activity and kinetics of enzymes involved in cellular processes (38), non-calcified cells might require extra energy to cope with the negative effect of decreased pH. The increment of chl *a* content in non-calcified cells (leading to increased light harvesting) might therefore provide extra energy to deal with the negative effect caused by elevated cytoplasmic H^+. However, the precise nature of how calcification may protect against acidification will require further work to understand what is involved in the loss of calcification in the non-calcifying strain.

PSII is susceptible to light, especially to high levels of PAR or UV radiation (39,40). The D1 protein is the primary target in PSII for UV photo-damage, and the balance between photo-damage and repair is a key determinant of the maintenance of photosynthesis (41). In the present study, the effective quantum yield showed similar final values ($P > 0.05$), and no significant difference in the *r:k* ratio ($P > 0.05$) was observed, under each light treatment for both cell types under LC conditions. This result is contrary to Xu *et al.* who measured the time course of effective quantum yield of calcified and non-calcified cells of *E. huxleyi* under solar light and found a remarkable difference, with the final effective quantum yield of naked cells lower than that of calcified cells (42). However, in their study, the calcified and non-calcified cells were from two different strains. As there is ample evidence of intra-specific differences in *E. huxleyi*, the different behavior might originate from genetic diversity (43–45). It is also possible that there are significant differences in the optical properties of *Gephryocapsa,* used in the present work, and those of the various *E. huxleyi* morphotypes (46–48).

NPQ is considered one of the most effective mechanisms for photo-protection (49). In the present study, NPQ was higher in non-calcified cells compared with calcified cells under each light treatment and the LC conditions. Gao *et al.* measured the transmission of radiation through decalcified and calcified cells and found a 20–25% decrease in UVR and a 10–22% decrease in PAR due to coccoliths (16), suggesting that coccoliths might play a protective role by scattering electro-magnetic radiation (including UVR). As is reflected in our results, calcified cells had a low damage rate compared with non-calcified cells especially under PAB treatment ($P < 0.05$). Thus, the higher NPQ might be caused by the higher light stress suffered in non-calcified cells. According to the evidence mentioned above, it is reasonable to conclude that although the calcification of calcified cells played a protective role against the stress caused by UV and PAR radiation, non-calcified cells could also cope with the stress, by adjusting their energy dissipation processes, such as by increasing NPQ.

Elevated pCO_2 exacerbated the effect of UV on the susceptibility of PSII in non-calcified cells, as the effective quantum yield decreased severely ($P < 0.05$) and NPQ increased (though changes were not statistically significant) under UV irradiance. Since the balance between photo-damage and repair is a key determinant of the maintenance of photosynthesis, and damage was not increased in non-calcified cells, this finding must originate from the significantly decreased repair capacity in non-calcified cells under HC conditions, as shown in Fig. 7. The potentially higher H^+ stress suffered by non-calcified cells (as discussed above) might act either directly through influencing the molecular mechanisms for the process of D1 protein renovation or indirectly through competing energy demands, as both H^+

extrusion and D1 protein repair are energy demanding processes. In addition, since previous studies have demonstrated that excess light energy absorbed by photosynthetic pigments can lead to accelerated photo-inhibition via inhibition of the repair of photo-damaged PSII (50), the reduced repair rate in non-calcified cells under each light treatment (especially under UVR) at elevated pCO_2 might also be due to the significant increment of pigment contents (Fig 4). This is consistent with the work of (51), who found *E. huxleyi* CS369 acclimated to solar light had a reduced pigment content and showed a higher repair capacity than cells grown under laboratory light. Although the PIC quotas significantly decreased, no significant difference of effective quantum yield was observed under each light treatment in calcified cells when transferred to HC conditions, whereas simultaneous changes of repair rate and damage rate were observed, ultimately leading to a constant *r*:*k* ratio. This suggests that although elevated pCO_2 led to a higher damage rate in calcified cells as well as in non-calcified cells, the calcified cells had more available energy (as discussed above) to cope with the stress by increasing their repair rate simultaneously to maintain photosynthesis. Compared with the study of Gao *et al.*, who found that ocean acidification led to a significant reduction of photosynthetic carbon fixation in calcified *E. huxleyi* CS369 under UV radiation (16), we inferred that the increased repair capability needed an enhanced allocation of energy and resources at the cost of decreased carbon fixation. However, Gao *et al.* reported that the increased UV susceptibility at elevated pCO_2 was caused by the thinner coccolith layer of cells grown under the acidified conditions (16). Since increased pCO_2 reduced the effective quantum yield in non-calcified cells and no significant influence of effective quantum yield was observed in calcified cells under UV irradiance in our study, we conclude that the negative impact of elevated cytoplasmic H^+ alone would exacerbate the detrimental effects of UV radiation while the possession of calcification attenuated this influence.

Acknowledgements—This study was supported by National Natural Science Foundation (41430967, 41720104005, 41721005), the NSFC - Shandong Joint Fund for Marine Ecology and Environmental Sciences (U1606404). JB's visit to Xiamen was supported by Xiamen University.

SUPPORTING INFORMATION

Additional supporting information may be found online in the Supporting Information section at the end of the article:

Table S1. Results of threeway ANOVAs of the effects of type, light, CO_2 and their interaction on *r*, *k* and *r*:*k* ratio.

REFERENCES

1. Mackinder, L., G. Wheeler, D. Schroeder, U. Riebesell and C. Brownlee (2010) Molecular mechanisms underlying calcification in coccolithophores. *Geomicrobiol J.* **27**, 585–595.
2. Paasche, E. (2001) A review of the coccolithophorid *Emiliania huxleyi* (Prymnesiophyceae), with particular reference to growth, coccolith formation, and calcification-photosynthesis interactions. *Phycologia* **40**, 503–529.
3. Raven, J. A. and K. Crawfurd (2012) Environmental controls on coccolithophore calcification. *Mar. Ecol. Prog. Ser.* **470**, 137–166.
4. Berry, L., A. R. Taylor, U. Lucken, K. P. Ryan and C. Brownlee (2002) Calcification and inorganic carbon acquisition in coccolithophores. *Funct. Plant Biol.* **29**, 289–299.
5. Monteiro, F. M., L. T. Bach, C. Brownlee, P. Bown, R. E. M. Rickaby, A. J. Poulton, T. Tyrrell, L. Beaufort, S. Dutkiewicz, S. Gibbs, M. A. Gutowska, R. Lee, U. Riebesell, J. Young and A. Ridgwell (2016) Why marine phytoplankton calcify. *Sci. Adv.* **2**, e1501822.
6. Meyer, J. and U. Riebesell (2015) Reviews and syntheses: Responses of coccolithophores to ocean acidification: A meta-analysis. *Biogeosciences* **12**, 1671–1682.
7. Nanninga, H. J. and T. Tyrrell (1996) Importance of light for the formation of algal blooms by *Emiliania huxleyi*. *Mar. Ecol. Prog. Ser.* **136**, 195–203.
8. Buma, A. G. J., T. Van Oijen, W. Van De Poll, M. J. W. Veldhuis and W. W. C. Gieskes (2000) The sensitivity of *Emiliania huxleyi* (Prymnesiophyceae) to ultraviolet-b radiation. *J. Phycol.* **36**, 296–303.
9. Sobrino, C., O. Montero and L. M. Lubián (2004) UV-B radiation increases cell permeability and damages nitrogen incorporation mechanisms in *Nannochloropsis gaditana*. *Aquat. Sci.* **66**, 421–429.
10. Xu, K., K. Gao, V. E. Villafañe and E. W. Helbling (2011) Photosynthetic responses of *Emiliania huxleyi* to UV radiation and elevated temperature: Roles of calcified coccoliths. *Biogeosciences* **8**, 1441–1452.
11. Guan, W. and K. Gao (2010) Enhanced calcification ameliorates the negative effects of UV radiation on photosynthesis in the calcifying phytoplankter *Emiliania huxleyi*. *Chinese Sci. Bull.* **55**, 588–593.
12. Gao, K., Z. Ruan, V. E. Villafañe, J.-P. Gattuso and E. W. Helbling (2009) Ocean acidification exacerbates the effect of UV radiation on the calcifying phytoplankter *Emiliania huxleyi*. *Limnol. Oceanogr.* **54**, 1855–1862.
13. Quintero-Torres, R., J. L. Aragón, M. Torres, M. Estrada and L. Cros (2006) Strong far-field coherent scattering of ultraviolet radiation by holococcolithophores. *Phys. Rev. E* **74**, 032901.
14. Sobrino, C., M. L. Ward and P. J. Neale (2008) Acclimation to elevated carbon dioxide and ultraviolet radiation in the diatom *Thalassiosira pseudonana*: Effects on growth, photosynthesis, and spectral sensitivity of photoinhibition. *Limnol. Oceanogr.* **53**, 494–505.
15. Klaveness, D. and E. Paasche (1971) Two different *Coccolithus huxleyi* cell types incapable of coccolith formation. *Archiv für Mikrobiol.* **75**, 382–385.
16. Bendif, E. M. and J. Young (2014) On the Ultrastructure of *Gephyrocapsa oceanica* (Haptophyta) Life Stages. *Cryptogamie Algol.* **39**, 379–388.
17. Morel, F. M. M., J. G. Rueter, D. M. Anderson and R. R. L. Guillard (1979) Aquil: A chemically defined phytoplankton culture medium for trace metal studies. *J. Phycol.* **15**, 135–141.
18. Lewis, E. and D. W. R. Wallace (1998) Program developed for CO_2 system calculations. ORNL/CDIAC-105, Carbon Dioxide Information Analysis Center, Oak Ridge National Laboratory, US Department of Energy. 20.
19. Roy, R. N., L. N. Roy, K. M. Vogel, C. Porter-Moore, T. Pearson, C. E. Good, F. J. Millero and D. M. Campbell (1993) The dissociation constants of carbonic acid in seawater at salinities 5 to 45 and temperatures 0 to 45°C. *Mar. Chem.* **44**, 249–267.
20. Heraud, P. and J. Beardall (2000) Changes in chlorophyll fluorescence during exposure of *Dunaliella tertiolecta* to UV radiation indicate a dynamic interaction between damage and repair processes. *Photosynth. Res.* **63**, 123–134.
21. Porra, R. J. (2005) The chequered history of the development and use of simultaneous equations for the accurate determination of chlorophylls a and b. In *Discoveries in Photosynthesis* (Edited by Govindjee, J. T. Beatty, H. Gest and J. F. Allen), pp. 633–640. Springer, Dordrecht, the Netherlands.
22. Ritchie, R. J. (2006) Consistent sets of spectrophotometric chlorophyll equations for acetone, methanol and ethanol solvents. *Photosynth. Res.* **89**, 27–41.
23. Strickland, J. D. H. and T. R. Parsons (1968) A practical handbook of seawater analysis. *Fish. Res. Board Can. Bull.* **167**, 49–80.
24. Rokitta, S. D. and B. Rost (2012) Effects of CO2 and their modulation by light in the life-cycle stages of the coccolithophore *Emiliania huxleyi*. *Limnol. Oceanogr.* **57**, 607–618.
25. Mausz, M. A. and G. Pohnert (2015) Phenotypic diversity of diploid and haploid *Emiliania huxleyi* cells and of cells in different growth

phases revealed by comparative metabolomics. *J. Plant Physiol.* **172**, 137–148.
26. Rokitta, S. D., L. J. de Nooijer, S. Trimborn, C. de Vargas, B. Rost and U. John (2011) Transcriptome analyses reveal differential gene expression patterns between life-cycle stages of *Emiliania huxleyi* (Haptophyta) and reflect specialization to different ecological niches. *J. Phycol.* **47**, 829–838.
27. Brady Olson, M., T. A. Wuori, B. A. Love and S. L. Strom (2017) Ocean acidification effects on haploid and diploid *Emiliania huxleyi* strains: Why changes in cell size matter. *J. Exp. Mar. Biol. Ecol.* **488**, 72–82.
28. Kottmeier, D. M., S. D. Rokitta and B. Rost (2016) Acidification, not carbonation, is the major regulator of carbon fluxes in the coccolithophore *Emiliania huxleyi*. *New Phytol.* **211**, 126–137.
29. Bach, L. T., L. C. Mackinder, K. G. Schulz, G. Wheeler, D. C. Schroeder, C. Brownlee and U. Riebesell (2013) Dissecting the impact of CO_2 and pH on the mechanisms of photosynthesis and calcification in the coccolithophore *Emiliania huxleyi*. *New Phytol.* **199**, 121–134.
30. Langer, G., G. Nehrke, I. Probert, J. Ly and P. Ziveri (2009) Strain-specific responses of *Emiliania huxleyi* to changing seawater carbonate chemistry. *Biogeosciences* **6**, 2637–2646.
31. Jin, P., K. Gao and J. Beardall (2013) Evolutionary responses of a coccolithophorid *Gephyrocapasa oceanica* to ocean acidification. *Evolution* **67**, 1869–1878.
32. Zhang, Y., L. T. Bach, K. G. Schulz and U. Riebesell (2015) The modulating effect of light intensity on the response of the coccolithophore *Gephyrocapsa oceanica* to ocean acidification. *Limnol. Oceanogr.* **60**, 2145–2157.
33. Diner, R. E., I. Benner, U. Passow, T. Komada, E. J. Carpenter and J. H. Stillman (2015) Negative effects of ocean acidification on calcification vary within the coccolithophore genus *Calcidiscus*. *Mar. Biol.* **162**, 1287–1305.
34. Suffrian, K., K. G. Schulz, M. A. Gutowska, U. Riebesell and M. Bleich (2011) Cellular pH measurements in *Emiliania huxleyi* reveal pronounced membrane proton permeability. *New Phytol.* **190**, 595–608.
35. Flynn, K. J., J. C. Blackford, M. E. Baird, J. A. Raven, D. R. Clark, J. Beardall, C. Brownlee, H. Fabian and G. L. Wheeler (2012) Changes in pH at the exterior surface of plankton with ocean acidification. *Nat. Clim. Change* **2**, 510–513.
36. Wolf-Gladrow, D. and U. Riebesell (1997) Diffusion and reactions in the vicinity of plankton: A refined model for inorganic carbon transport. *Mari. Chem.* **59**, 17–34.
37. Michelle, S. H. and G. M. James (2001) Functional morphology of diatom frustule microstructures: Hydrodynamic control of Brownian particle diffusion and advection. *Aquat. Microb. Ecol.* **24**, 287–295.
38. Badger, M. (2003) The roles of carbonic anhydrases in photosynthetic CO_2 concentrating mechanisms. *Photosynth. Res.* **77**, 83.
39. Campbell, D. A. and E. Tyystjärvi (2012) Parameterization of photosystem II photoinactivation and repair. *BBA – Bioenergetics* **1817**, 258–265.
40. Long, S. P., S. Humphriesh and P. G. Falkowski (1994) Photoinhibition of photosynthesis in nature. *Ann. Rev. Plant Physiol. Plant Mol. Biol.* **45**, 633–662.
41. Wu, Y., Z. Li, W. Du and K. Gao (2015) Physiological response of marine centric diatoms to ultraviolet radiation, with special reference to cell size. *J. Photochem. Photobiol., B* **153**, 1–6.
42. Xu, J., L. T. Bach, K. G. Schulz, W. Zhao, K. Gao and U. Riebesell (2016) The role of coccoliths in protecting *Emiliania huxleyi* against stressful light and UV radiation. *Biogeosciences* **13**, 4637–4643.
43. Young, J. R. and P. Westbroek (1991) Genotypic variation in the coccolithophorid species *Emiliania huxleyi*. *Mar. Micropaleontol.* **18**, 5–23.
44. Kegel, J. U., U. John, K. Valentin and S. Frickenhaus (2013) Genome variations associated with viral susceptibility and calcification in *Emiliania huxleyi*. *PLoS ONE* **8**, e80684.
45. von Dassow, P., U. John, H. Ogata, I. Probert, E. M. Bendif, J. U. Kegel, S. Audic, P. Wincker, C. Da Silva, J.-M. Claverie, S. Doney, D. M. Glover, D. M. Flores, Y. Herrera, M. Lescot, M.-J. Garet-Delmas and C. de Vargas (2014) Life-cycle modification in open oceans accounts for genome variability in a cosmopolitan phytoplankton. *ISME J.* **9**, 1365.
46. Young, J. R., S. A. Davis, P. R. Bown and S. Mann (1999) Coccolith ultrastructure and biomineralisation. *J. Struct. Biol.* **126**, 195–215.
47. Young, J. R. (2003) Biomineralization within vesicles: The calcite of coccoliths. *Rev. Mineral. Geochem.* **54**, 189–215.
48. Bendif, E. M., I. Probert, F. Díaz-Rosas, D. Thomas, G. van den Engh, J. R. Young and P. von Dassow (2016) Recent reticulate evolution in the ecologically dominant lineage of coccolithophores. *Front. Microbiol.* **7**, 784.
49. Muller, P., X. Li and K. K. Niyogi (2001) Non-photochemical quenching. a response to excess light energy. *Plant Physiol.* **125**, 1558–1566.
50. Nishiyama, Y., S. I. Allakhverdiev and N. Murata (2006) A new paradigm for the action of reactive oxygen species in the photoinhibition of photosystem II. *BBA – Bioenergetics* **1757**, 742–749.
51. Xing, T., K. Gao and J. Beardall (2015) Response of growth and photosynthesis of *Emiliania huxleyi* to visible and UV irradiances under different light regimes. *Photoch. Photobiol. B.* **91**, 343–349.